DESIGN, CONSTRUCTION AND TEST OF A FULL SCALE SSC DIPOLE MAGNET CRYOSTAT THERMAL MODEL

R. C. Niemann, J. A. Carson, N. H. Engler, J. D. Gonczy,
T. H. Nicol, J. G. Otavka, R. J. Powers and J. C. Theilacker
Fermi National Accelerator Laboratory,†
P.O. Box 500
Batavia, Illinois 60510

Abstract

As a part of the SSC main ring superconducting magnet development program, a full length dipole magnet thermal model has been constructed and its thermal performance measured. Presented are the details of the cryostat design and the thermal model construction experience and its evaluation. The methods for and the preliminary results of the thermal performance measurements are presented and compared with the predicted performance.

Introduction

As a part of the SSC superconducting magnet development program, a series of full length dipole magnet models has been designed by BNL, Fermilab and LBL, and is being constructed. As a precursor to the construction of the actual magnet models, a full length (17.5m) thermal model was built.

The objectives of the thermal model program were to utilize and improve the cryostat production facility and manufacturing procedures, to evaluate the cryostat design from a production standpoint, to gain experience in handling and transportation, and to measure the heat leaks to the thermal shields and the cold mass.

The thermal model is identical to magnet models except that the cold mass assembly contains a simulated collared coil assembly. The cryostat has been instrumented to evaluate thermal and structural performance. Included are temperature sensors to monitor cooldown, warmup and steady state conditions and strain gauges to monitor the performance of the suspension system during onsite transit, cooldown and operation. Construction of the thermal model employs the fabrication facility, procedures and the components for the actual models.

Cryostat Design

The cryostat design has been described in detail previously[1,2] and thus only its major features are presented herein.

The cryostat cross section is as shown by Fig. 1. The major elements are the cold mass assembly, cryogenic piping, thermal shields, suspension system, insulation, vacuum vessel and interconnections.

Cold Mass Assembly

The cold mass assembly consists of the beam tube, correction elements, collared coils, laminated iron yoke and outer helium containment shell joined together to provide a leak-tight and structurally rigid welded assembly. The helium containment shell is the principal structural element and provides rigidity between suspension points.

†Operated by Universities Research Assn. Inc., under contract with the U.S. Department of Energy.

Manuscript received September 30, 1986.

Cryogenic Piping

The cryostat contains all piping that interconnects the magnet refrigeration system throughout the circumference of the ring. A system consisting of five pipes was selected for cryogenic and magnet safety reasons. The pipes are the cold mass assembly, the helium fluid return and recooler supply pipe, the helium gas return pipe, the 20K helium shield cooling pipe and the 80K liquid nitrogen shield cooling pipe.

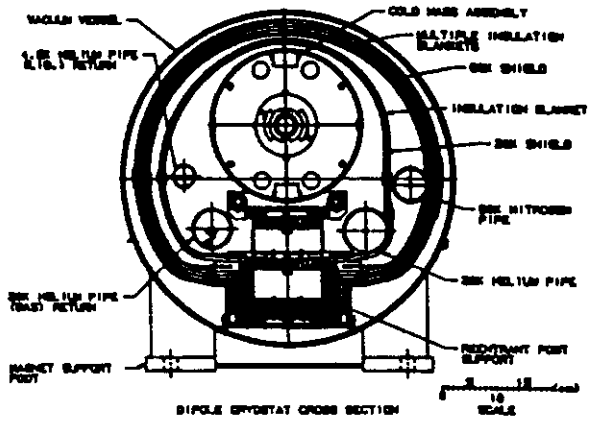

Figure 1. Dipole magnet cross section at a support location.

Thermal Shields

Thermal shields maintained independently at 20 and 80K surround the cold mass assembly. The shields absorb the radiant heat flux and provide heat sink stations for the suspension system. The shields, constructed of aluminum, are supported by and thermally connected to the cold mass assembly supports.

The liquid and gaseous helium return pipes are supported from the cold mass assembly by hangers.

Suspension System

The cold mass and shields are supported relative to the vacuum vessel by the suspension system.[3] The system functions under conditions that include assembly, transportation and installation, magnet cooldown and warmup, and magnet steady-state and transient conditions.

The cold mass and shields are supported at five points. The number and location of the support points were determined by cold mass deflection and by the need to minimize the number of support points for reasons of fabrication and heat leak.

The suspension incorporates a reentrant type post support. The support's insulating sections are fiber reinforced plastic (FRP) tubing with metallic connections and heat intercepts. The FRP to metallic junctions are made by shrink fitting. Control of

Presented at the 1986 Applied Superconductivity Conference
held in Baltimore, Maryland September 28 - October 3, 1986

internal thermal radiation is by the use of multilayer insulation. A support mounted to the cold mass with shield thermal connections during construction is as shown by Fig. 2.

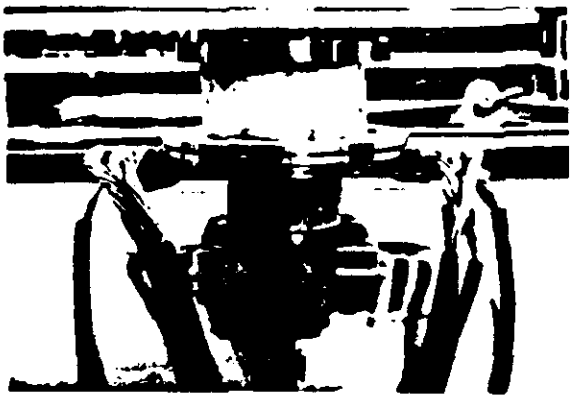

Figure 2. Installation of support assembly on cold mass assembly. Cables provide thermal linkage between shields and support intercept stations.

The support post is fixed at the warm end and incorporates a slide at the cold end to allow axial differential contraction between the mid-span anchored cold mass and vacuum vessel.

To permit the support to survive the lateral handling loads without incurring a severe operational heat leak penalty, the support post incorporates an integral, coaxial, removable shipping restraint.

Efficient thermal connections between the 20 and 80K intercepts and the shields are essential to reduce heat leak. A 5K temperature rise at 80K and a 1K temperature rise at 20K are budgeted.

The cryostat employs removable axial shipping restraints which provide strong axial connection between the cold mass and the vacuum vessel.

Insulation

Insulation is installed on the 20 and 80K surfaces. The insulation consists of prefabricated blankets of flat, reflective radiation shields of aluminized polyester film with mat spacers of randomly oriented fiberglass. Each blanket contains 13 reflective layers and has a thickness of ~0.64cm. One blanket is installed on the 20K surface and four are installed on the 80K surface.

Vacuum Vessel

The vacuum vessel provides the insulating vacuum space and the connection of the suspension system to ground. Since the vessel has no magnetic requirements, candidate materials were carbon steel, stainless steel, 9% nickel steel and aluminum. Carbon steel was selected on the basis of cost.

Interconnections

Mechanical and electrical interconnections are required at the magnet ends. It is essential that the connections be straightforward to assemble and disassemble, compact and reliable. The interconnection design facilitates assembly and disassembly operations in the SSC tunnel. The geometry permits the use of automated welding and cutting equipment that is essential for installation efficiency and interconnection reliability.

Thermal Model Construction

The cryostat thermal model is identical to an actual magnet with the following exceptions:

- The collared coil assembly is simulated.
- The ends are configured for open cycle heat leak measurement.
- Instrumentation is added for temperature and strain measurement and for calibration.

The cold mass assembly during construction is as shown by Fig. 3.

Figure 3. Cold mass assembly during construction. The simulated collared coil assembly is equipped with temperature sensors and calibration heaters.

The construction procedure involves parallel construction of the internal assembly and the vacuum vessel assembly followed by insertion of the internal assembly into the vacuum vessel.

Internal Assembly

The cold mass assembly is located on an assembly station. The suspension system slide cradles with attached support subassemblies are installed as shown by Fig. 2. The axial anchor subassembly and helium return lines are attached as shown by Fig. 4. The 20 and 80K shields are installed in sections to the support heat intercepts. The heat conduction straps are connected to the shields followed by the insulation blankets. The complete internal assembly is ready for insertion into the vacuum vessel.

Vacuum Vessel Assembly

The vacuum vessel has precision mounting feet which provide the alignment of the cold mass with respect to the vacuum vessel. End rings to hold shipping restraints and reinforcing segments at the support points are attached.

Insertion

The completed vacuum assembly is transferred to the final assembly station and secured. A slide and winch system is used to pull the cold mass into the vacuum vessel. Precision fixture points together with the precise location of the support feet locate the internal assembly relative to the vacuum vessel.

The cold mass assembly is bolted to the vacuum vessel at the bottom of the support posts and the support post shipping restraints are installed. The magnet is inspected and the end axial shipping restraints are installed. The completed center section of the thermal model is shown by Fig. 5.

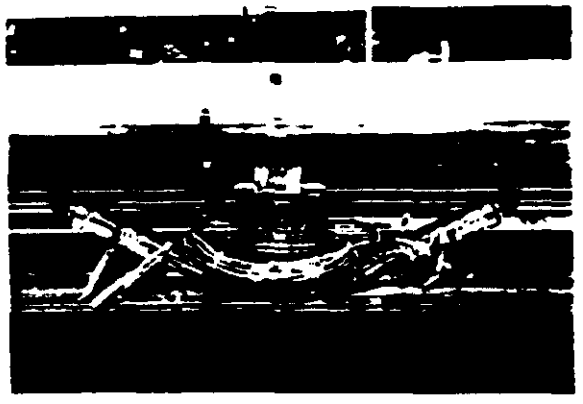

Figure 4. Midspan support point with support post and anchor assemblies. Helium return piping is in the background.

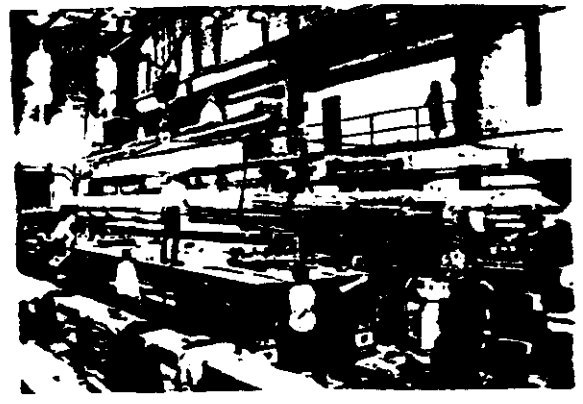

Figure 5. The completed thermal model center section being loaded for shipment to the heat leak measurement facility.

Conclusions

The construction of the thermal model progressed smoothly using the "as designed" components, tooling and procedures. The assembly experience resulted in an improved understanding of the production process as it would be applied to the construction of an actual SSC dipole magnet. The major conclusions resulting from the initial production experience are as follow:

- The construction of the model was, at times, impeded by complicated subassemblies, inadequate clearance between components, distortion due to welding, etc. The design is being improved in these areas with regard to function and produceability.
- The design lends itself to mass production:
  - Components from a variety of sources
  - Subsystem preassembly and inspection
  - Subsystem transfer between work stations
  - Assembly, alignment and inspection with specialized tooling
- High quality can be achieved with "as procured" components, production assembly procedures and tooling and production travelers.
- The "slide in" assembly method works well.

Thermal Performance Measurements

Test Method

The measurements were made in an open cycle mode with liquid helium and liquid nitrogen supplied by reservoirs at each end and the inner shield cooled by means of an independent helium dewar. The measurement system schematic is shown by Fig. 6.

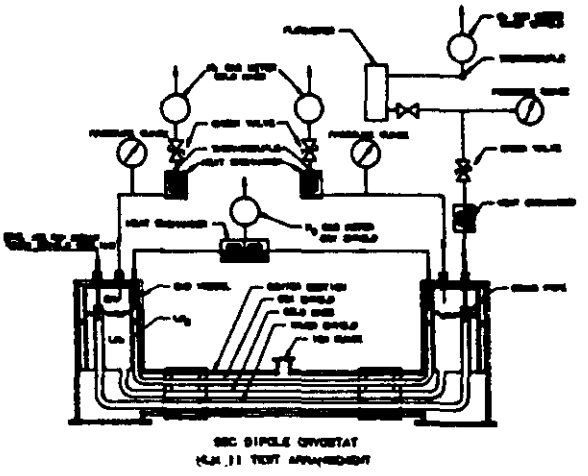

Figure 6. Thermal model measurement schematic.

The 80K heat leak was determined by measuring nitrogen boiloff.

The 20K heat leak was determined by measuring the mass flow rate and temperature rise of the helium gas flowing through the inner shield cooling pipe.

The 4.5K heat leak was determined by two methods; by measuring the helium boiloff and by measuring the temperature rate of rise of the simulated cold mass.

The background heat leak to 80K of 23.3W, was measured with the two end vessels connected together. The background heat leak to 4.5K of 865mW, was measured with the inner shield cooled with 5K liquid helium.

The operation of the system with the exception of the gas flowmeters, pressure gauges and vacuum monitors was monitored with an on line computer based data acquisition system.

Cooldown

Cooldown was gradual due to the open cycle nature of the apparatus and the low pressures employed. The cold mass was cooled and filled with liquid nitrogen, evacuated and then filled with liquid helium. The total time required to fill the cold mass with liquid helium was 294 hrs.

The post bending loads due to differential axial thermal contraction were low with the exception of the downstream end post which indicated a load of 4800N. The most probable cause for such a load is a nonoperational cold mass slide.

The temperature distribution of the support posts agreed well with that of an identical post measured in a heat leak measurement dewar.[6]

Random mechanical noises occurred in the cryostat during cooldown and through the entire measurement period which lasted several months. A probable cause of such noises is relative motion between the cold mass and/or shields and support posts that result from vacuum vessel motions due to ambient temperature variations and/or settling of the concrete test pad.

Predicted Heat Leaks

The predicted heat leaks to the 80 and 20K shields and cold mass at the cryostat design point; i.e., inner shield at 20K, are given by Table 1. The predictions were analytical in nature and in the case of the supports were verified by measurement.[7,8]

Table 1. Thermal Model Predicted Heat Leak

Heat Leak Component	Heat Leak to Temperature[1,2] [W] 80K	20K	4.5K
. Cold Mass Supports	5.66	0.610	.065
. Cold Mass Anchor	0.83	0.071	.015
. Thermal Radiation	16.47	1.982	.005
. Residual Gas Conduction	0.31	0.111	.043
	23.27	2.774	0.128

1. For center section only.
2. With inner shield at 20K.

Results

The heat leak measurement data taking has been recently completed and the initial screening of the data performed. Final screening and corrections are underway and will be complemented by an error analysis.

The heat leak values are the results of many data points taken over several measurement runs. The raw data has been screened on the basis of center section thermal equilibrium time, end vessel stability, transfer operations, etc. The results were derived by averaging the screened data points. The preliminary heat leak measurements are presented in the following paragraphs.

Preliminary 80K Heat Leak Measurement

The preliminary 80K heat leak at the cryostat design point was 20.3W as compared to the predicted 23.3W. The preliminary 80K heat leak vs inner shield temperature data is given by Figure 7. The predicted 80K heat leak is plotted for reference.

Preliminary 20K Heat Leak Measurement

The preliminary 20K heat leak at the cryostat design point was 4.98W as compared to the predicted 2.77W. The 20K preliminary heat leak vs inner shield temperature data is given by Fig. 8. The predicted 20K heat leak is plotted for reference.

An approximate corroboration of the 20K heat leak measurement was provided by shield boiloff measurements that occurred during the cold mass "background" measurement. With the shield cooling tube filled with liquid helium, the heat leak as measured by boiloff was 5.64 W. The boiloff measurement includes end effects.

The approximate factor of two difference in measured over predicted heat leak is felt to be due to thermal shorts between the 80 and 20K systems and by locally compressed insulation between the shields. Shield and support temperature monitors indicate the possibility of shorts. The existence of such shorts is believable due to close fits between the 80 and 20K components in certain areas of the cryostat cross section.

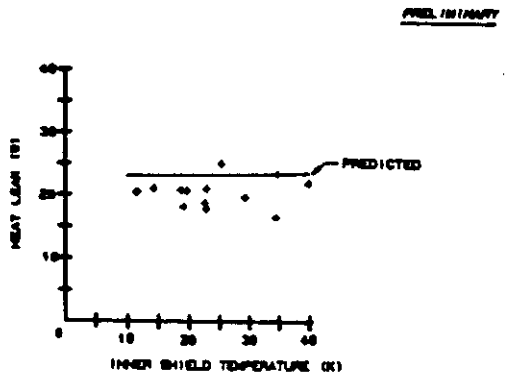

Figure 7. Preliminary measured 80K heat leak vs inner shield temperature.

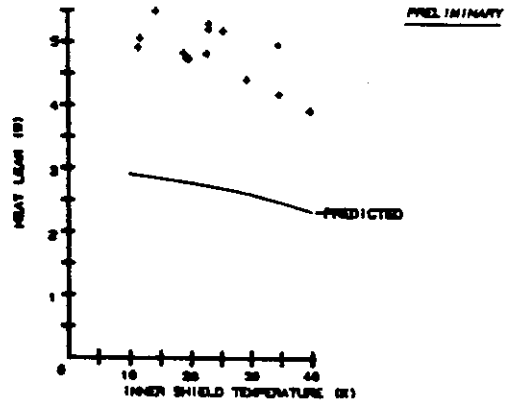

Figure 8. Preliminary measured 20K heat leak vs inner shield temperature.

Preliminary Cold Mass Heat Leak Measurements

The preliminary cold mass heat leak, by boiloff at the cryostat design point was 172mW as compared to the predicted 128mW. The cold mass preliminary heat leak vs inner shield temperature is given by Fig. 9. The predicted cold mass heat leak is plotted for reference.

As shown by Figure 9, sizeable discrepancies exist between the measured and predicted heat leaks at several experimental points. The factors that contribute to these discrepancies are as follow:

. The center section heat leak is small relative to the balance of the apparatus; i.e., ~172mW

vs 865mW, which results in an amplification of effects that occur in the end vessels.

- Thermal communication exists between the 20K cooling circuit and the end vessel helium reservoirs.
- Level instability occurred occasionally in the end vessels which resulted in sloshing. Sloshing adds energy to the liquid. The sloshing was most often associated with changes in the 20K circuit operation.
- The predicted sensitivity to insulating vacuum is high; i.e., at the 20K system operating point, the residual gas (helium) conduction at 10^{-8} torr is 83mW and at 10^{-5} torr is 430mW. The measured insulating vacuum at the vacuum vessel midspan port ranged from 1.3×10^{-6} to 2.9×10^{-6} torr during the span of the measurements. The location and installation of the vacuum gauge was demonstrated by measurements to not accurately relate changes in the insulating vacuum that could correspond to changes in the outgasing rate of the mild steel vacuum vessel as a result of changes of ambient temperature. The vacuum was not monitored frequently during most of the data taking.
- Variations in atmospheric pressure result in temperature changes of the liquid which influence the apparent heat leak. Atmospheric pressure was not monitored frequently during most of the data taking. The end to end cold mass temperature variations during running were characteristically ±30mK.

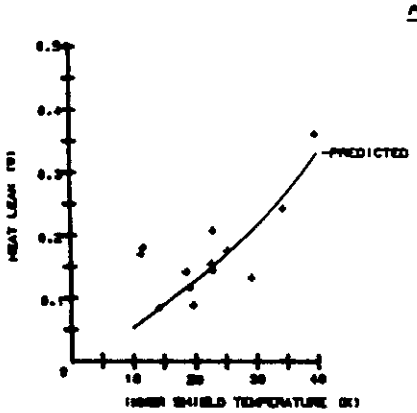

Figure 9. Preliminary measured cold mass heat leak vs inner shield temperature.

Calibration heaters on the simulated collared coil assembly were employed to evaluate the accuracy of the measurement of the heat leak to the cold mass. The heaters were energized with the inner shield at ~20K. The measured heat leak increases corresponding to heater power levels of 200mW and 398mW were 197mW and 376mW, respectively.

The cold mass heat leak measurement can be improved in several ways:

- Reduce background by using low heat leak end vessels.
- Reduce the thermal communication between the 20 and 4.5K circuits in the end vessels.
- Increase throughput to the vacuum space, improve vacuum and pressure mounting, and revise data acquisition protocol.
- Measure the heat leak of a string of magnets.

The measurement of the cold mass heat leak by the temperature rate of rise method remains to be done.

Conclusions

- The cryostat components, with the probable exception of the cold mass slides, performed well during cooldown and steady state operation. The cold mass slides have been improved for subsequent models as a result of this experience.
- The measurement methods for 80 and 20K are appropriate.
- With the exception of 20K, the measured heat leaks were within budget. The model's temperature monitors indicated possible shorts between the 20 and 80K systems. These shorts are associated with close fits in certain areas of the shield assemblies which compress the insulation and could cause direct contact between 20 and 80K components. These conditions are being improved in subsequent models.
- The measurement of the cold mass heat leak by boiloff methods for a single cryostat was difficult due to its small magnitude (172mW) as compared to the large background heat leak (865mW) associated with the end vessels, etc.
- The thermal measurements indicate that the superconducting magnets for the SSC can be built within the heat leak budgets as required by refrigeration system capital and operating costs of the accelerator.

Acknowledgements

The authors gratefully acknowledge the sincere interest, extensive contributions and diligent performance of the many Fermilab Technical Support design, magnet production and engineering test personnel. Their combined efforts resulted in the design, construction and test of a dipole magnet cryostat that corresponds to the cryogenic needs of the SSC.

References

1. R. C. Niemann, et al., "The Cryostat for the SSC 6 T Magnet Option," Adv. Cryo. Engr., 31, (1986) Plenum Press, New York.

2. SSC Central Design Group, "Conceptual Design of the Superconducting Super Collider," SSC-SR-2020, March 1986.

3. T. H. Nicol, et al., "A Suspension System for Superconducting Super Collider Magnet," Proceedings of the Eleventh International Cryogenic Engineering Conference, (1986)(to be published).

4. J. D. Gonczy, et al., "Heat Leak Measurement Facility," Adv. Cryo. Engr., 31, (1986) Plenum Press, New York.

5. M. Kuchnir, et al., "Measuring Heat Leak with a Heatmeter," Adv. Cryo. Engr., 31, (1986) Plenum Press, New York.